Detection of hot gas in distant (z>1.5) structures
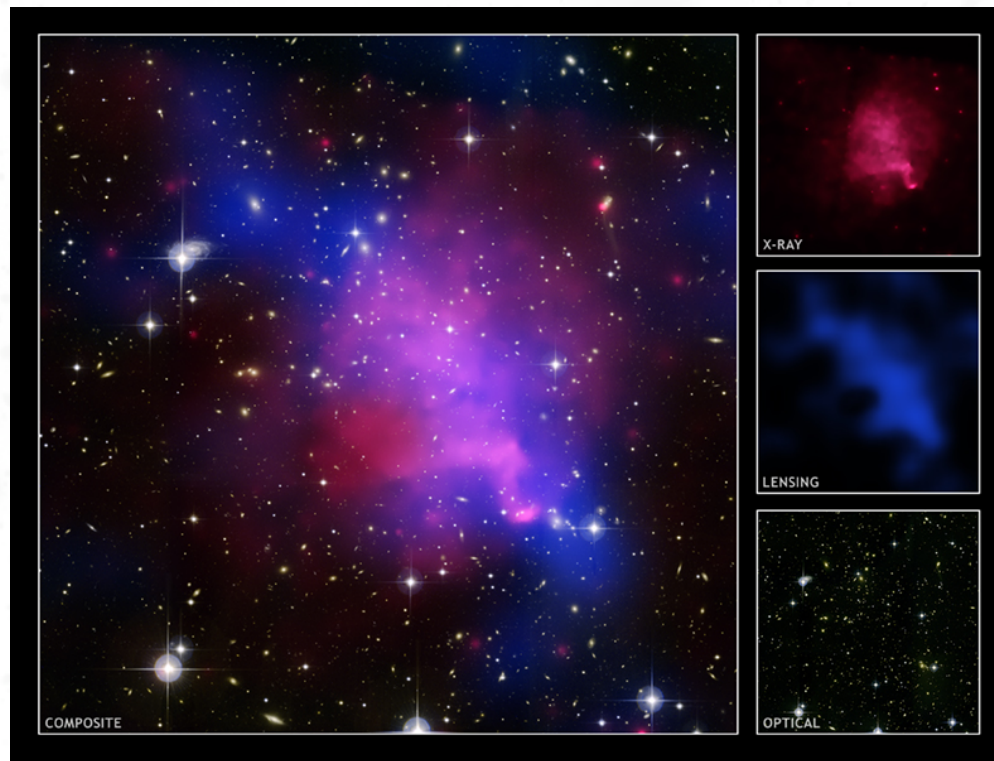
Loïc Verdier

CEA Saclay

December 2014
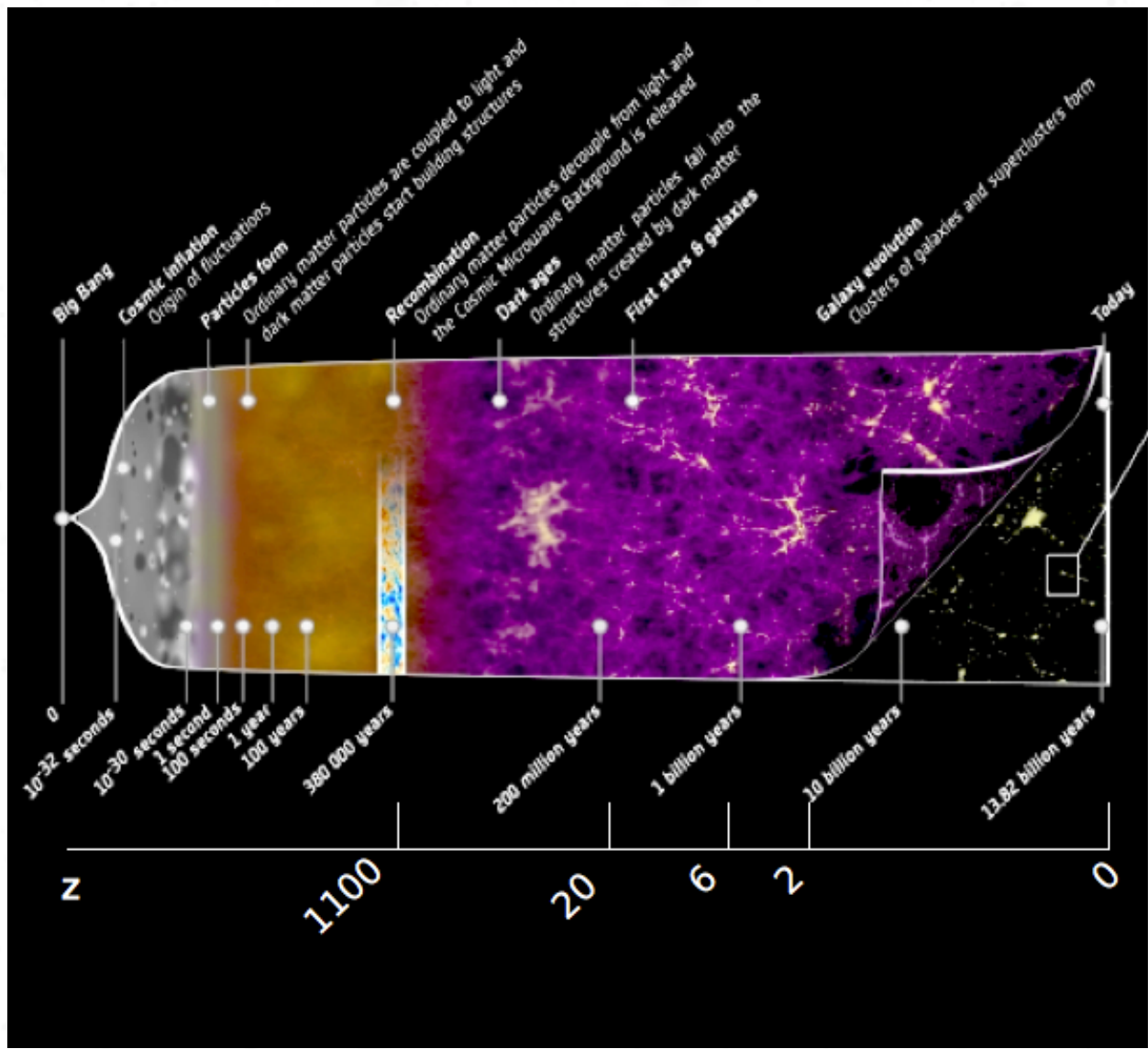
Cluster Abell 520; Credit: X-ray: NASA/CXC/UVic./A.Mahdavi et al. Optical/Lensing: CFHT/UVic./A.Mahdavi et al.
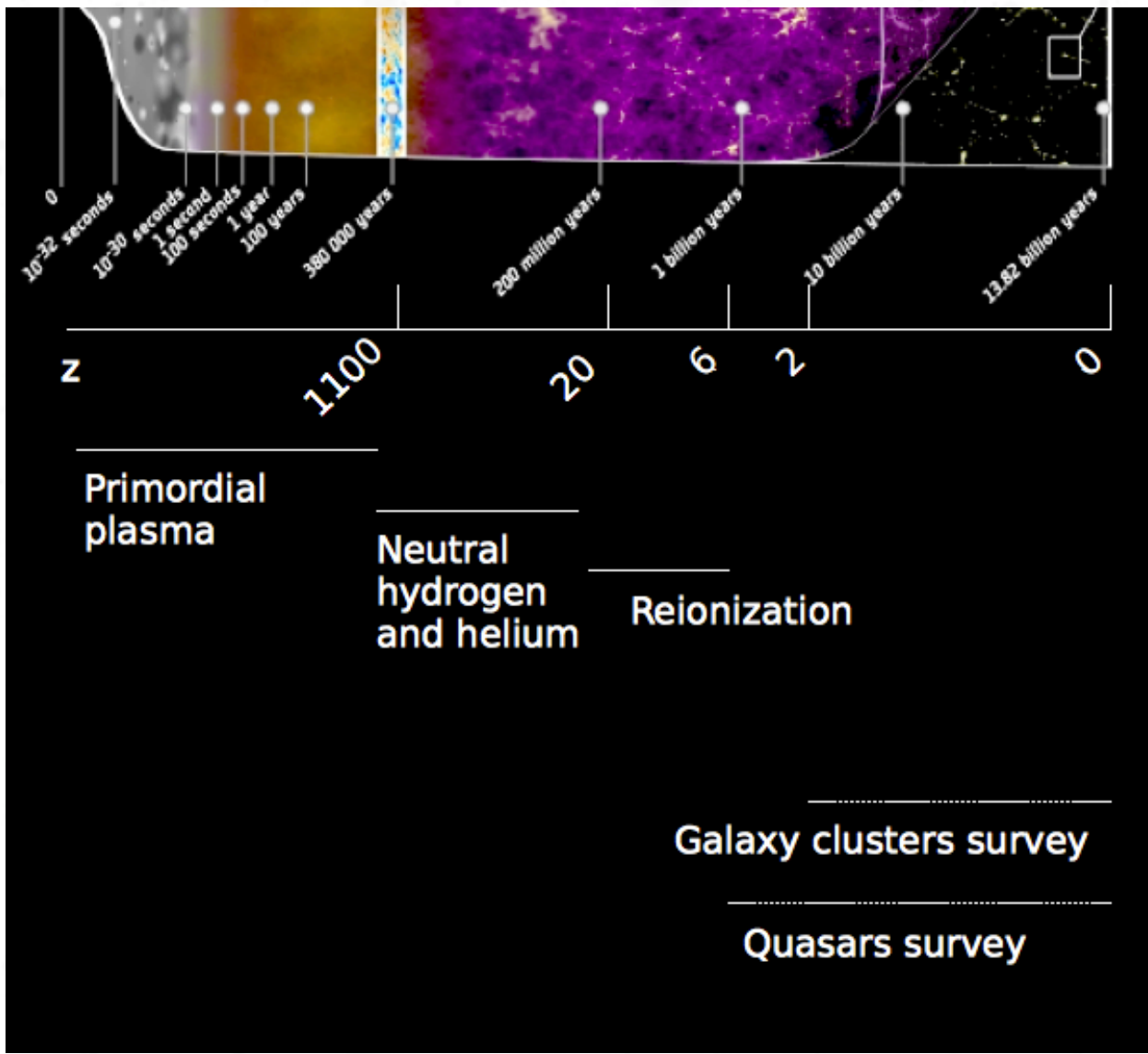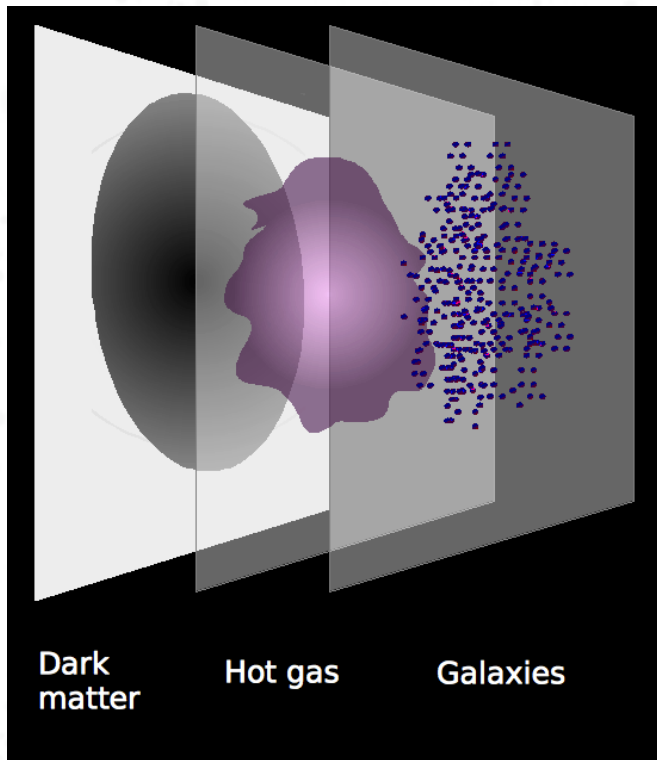
Table of contents

Story of the universe at different redshift

Story of the universe at different redshift; hot gas reappears during the reionization era.

Table of contents

Hot gas and clusters

Dark matter   Hot gas   Galaxies

Dark matter haloes and their baryonic contents

Primordial fluctuations of dark matter evolve in denser structures called haloes trough gravitational collapse. The baryonic matter is expected to follow closely the dark matter distribution. We define a **cluster** as the set of a dark matter halo, a diffuse hot gas and several galaxies. Here is the typical proportion of these different components:

- 85-88 % of dark matter
- 10-12 % of a **baryonic hot gas**.
- 2-3% of baryonic matter in galaxies.

Clusters have typical masses of $10^{14} M_\odot$ and typical radii around 10^{23} m (10^7 al)

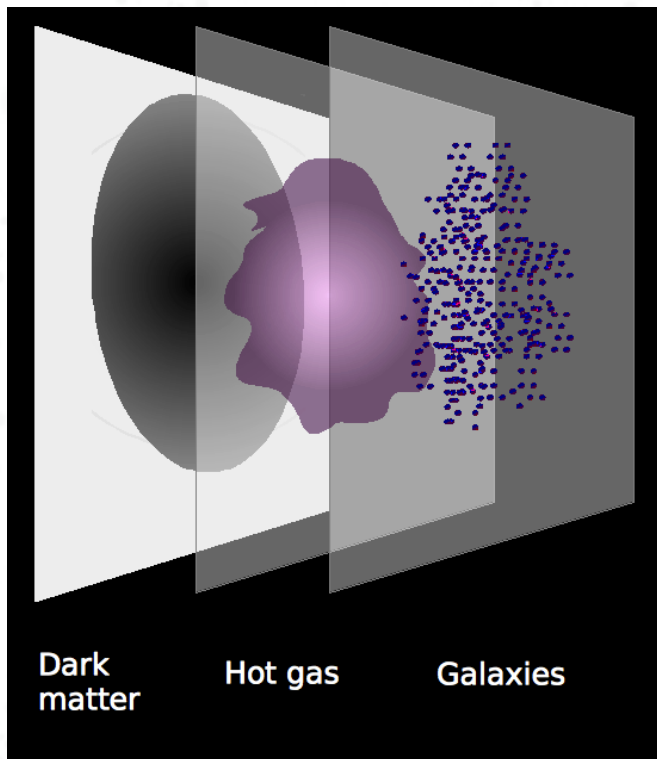# Hot gas and clusters

Dark matter   Hot gas   Galaxies

Dark matter haloes and their baryonic contents

Primordial fluctuations of dark matter evolve in denser structures called haloes trough gravitational collapse. The baryonic matter is expected to follow closely the dark matter distribution. We define a **cluster** as the set of a dark matter halo, a diffuse hot gas and several galaxies. Here is the typical proportion of these different components:

- 85-88 % of dark matter
- 10-12 % of a **baryonic hot gas**.
- 2-3% of baryonic matter in galaxies.

Clusters have typical masses of $10^{14}M_\odot$ and typical radii around 10^{23} m (10^7 al)

Hot gas properties

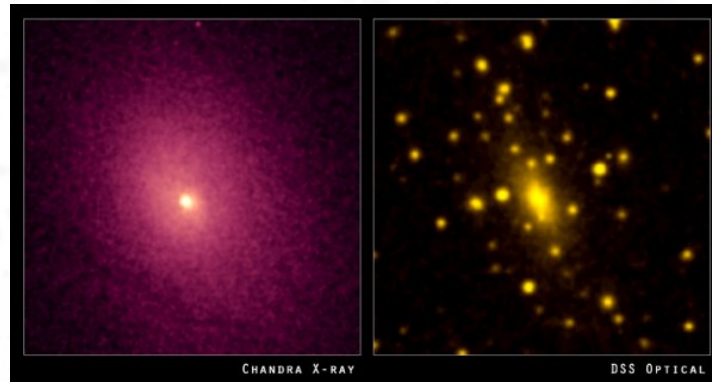The intra cluster medium (ICM), the area between the galaxies, is filled with hot gas having the following properties:

- Components: mainly ionized hydrogen and a small fraction of ionized helium.
- Electronic temperature: from $T \sim 1 \cdot 10^7 K$ to $T \sim 1 \cdot 10^8 K$.
- Average density: $\rho \sim 10^{-3}$ particles per cm^3. The gas is more diffuse on the halo's borders.

Table of contents

How to detect clusters?

The X-ray emission from the hot gas inside Abell 2029 (left) and the optical galaxies counterpart (right)

Using galaxies

Galaxies are mainly detected in optical. Galaxies over densities are interpreted as clusters. In many case, optical serve as a follow-up for detection at other wavelengths. The cluster redshifts are derived from the spectra of the galaxies.
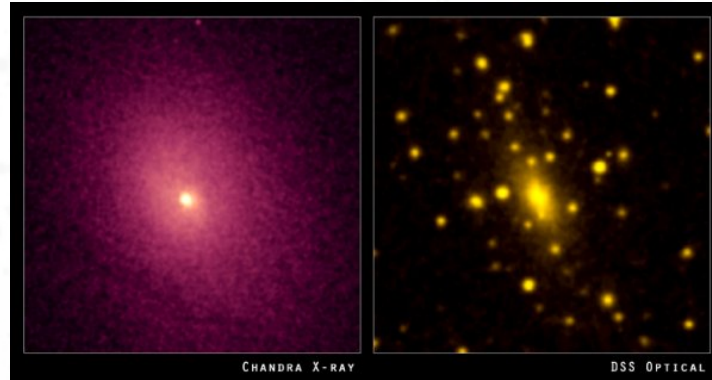
How to detect clusters?

The X-ray emission from the hot gas inside Abell 2029 (left) and the optical galaxies counterpart (right)

Using galaxies

Galaxies are mainly detected in optical. Galaxies over-densities are interpreted as clusters. In many case, optical serve as a follow-up for detection at other wavelengths. The cluster redshifts are derived from the spectra of the galaxies.

Using gravitational lensing

Mass curves the space-time and modify the trajectory of the light. Clusters of galaxies as massive structures act as lenses for the background sources. The deformation of this sources due to the gravitational lensing effect allows to estimate the **total mass of the cluster** (dark matter and baryonic matter).

How to detect clusters?

The X-ray emission from the hot gas inside Abell 2029 (left) and the optical galaxies counterpart (right)
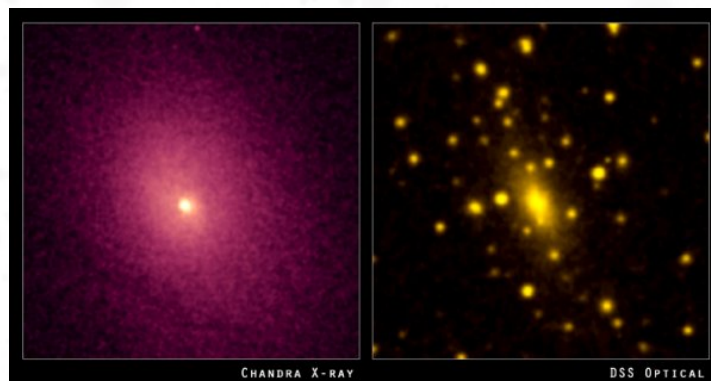
Using galaxies

Galaxies are mainly detected in optical. Galaxies over densities are interpreted as clusters. In many case, optical serve as a follow-up for detection at other wavelengths. The cluster redshifts are derived from the spectra of the galaxies.

Using gravitational lensing

Mass curves the space-time and modify the trajectory of the light. Clusters of galaxies as massive structures act as lenses for the background sources. The deformation of this sources due to the gravitational lensing effect allows to estimate the **total mass of the cluster** (dark matter and baryonic matter).

Using hot gas

Hot gas can be detected through two effects in two different wavelength ranges:

- in X-ray by **Bremsstrahlung**, the deceleration of the electrons. Specific missions: XMM, Chandra...
- in the millimeter wavelength range by **Sunyaev-Zel'dovich effect**, the interaction of CMB photons with the hot gas. Specific mission: Planck, SPT...

X-ray and SZ can probe the total mass of the clusters but cannot constraint the redshift.
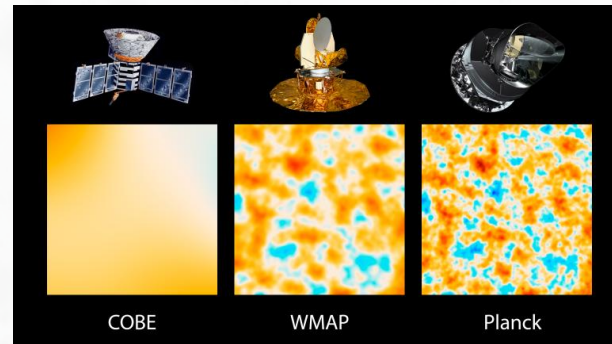
Table of contents

The Planck cluster survey (z<1)

Planck Mission

Dates: May 2009 - October 2013. But data still in processing. Planck satellite hosts the coolest objects in our nearby space: the bolometers refrigerated by Helium down to $T \sim 0.1K$. Among other things, Planck satellite was designed to detect the Cosmic Microwave Background (CMB) anisotropies as the third generation of millimeter wavelength range satellite after COBE (primordial fluctuations in the CMB) and WMAP(precise measure of the power spectrum). It is the first with enough resolution and sensitivity to detect many galaxy clusters via the Sunyaev-Zel'dovich effect. It hosts two instruments which measure **the flux** over the whole sky at **different frequencies**:

- HFI (High-frequency instrument): 100 GHz, 143 GHz, 217 GHz, 353 GHz, 545 GHz and 857 GHz.
- LFI (Low-frequency instrument): 30 GHz, 44 GHz and 70 GHz.

Links: http://www.cosmos.esa.int/web/planck
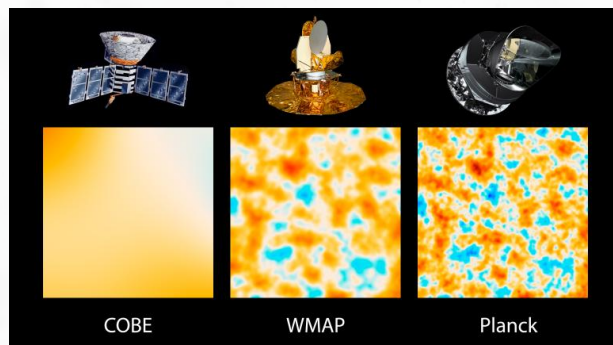

Planck resolution compared to its predecessors.

The Planck cluster survey (z<1)

Planck Mission

Dates: May 2009 - October 2013. But data still in processing. Planck satellite hosts the coolest objects in our nearby space: the bolometers refrigerated by Helium down to $T \sim 0.1K$. Among other things, Planck satellite was designed to detect the Cosmic Microwave Background (CMB) anisotropies as the third generation of millimeter wavelength range satellite after COBE (primordial fluctuations in the CMB) and WMAP (precise measure of the power spectrum). It is the first with enough resolution and sensitivity to detect many galaxy clusters via the Sunyaev-Zel'dovich effect. It hosts two instruments which measure **the flux** over the whole sky at **different frequencies**:

- HFI (High-frequency instrument): 100 GHz, 143 GHz, 217 GHz, 353 GHz, 545 GHz and 857 GHz.
- LFI (Low-frequency instrument): 30 GHz, 44 GHz and 70 GHz.

Links: http://www.cosmos.esa.int/web/planck

Planck resolution compared to its predecessors.

Clusters catalogue

The Planck clusters catalogue contains 1227 clusters and 861 have a counterpart (X-ray or optical). From the catalogue, we derive a **distribution of the clusters** as a function of redshift up to z=1 to constrain cosmology. Clusters and Sunyaev-Zel'dovich effect are a source of systematics for the CMB measurement. In the other perspective, CMB is a source of noise for the cluster detection. Links: http://fr.arxiv.org/abs/1303.5089

The new version of the Planck catalogue will contain 1651 clusters and 1110 with a counterpart (publication on Dec 22, 2014)

Table of contents

Detection of hot gas at higher redshift (z>1)

Individual detection at low redshift

Individual detection of clusters is possible for low-redshift structures via the X-ray Bremsstrahlung and the millimeter wavelength Sunyaev-Zel'dovich effect. Some actual limits:

- millimeter wavelength: SPT survey: detection of clusters up to z=1.5
- X-ray: Chandra confirmed a cluster at z=1.8 Links: http://arxiv.org/abs/1311.4361

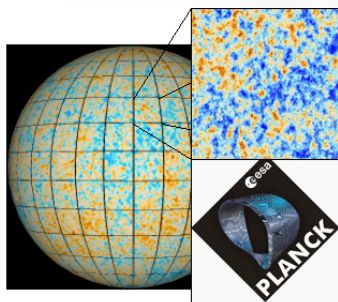# Detection of hot gas at higher redshift (z>1)

Individual detection at low redshift

Individual detection of clusters is possible for low-redshift structures via the X-ray Bremsstrahlung and the millimeter wavelength Sunyaev-Zel'dovich effect. Some actual limits:

- millimeter wavelength: SPT survey: detection of clusters up to z=1.5
- X-ray: Chandra confirmed a cluster at z=1.8 Links: http://arxiv.org/abs/1311.4361

More distant structures

In the standard model of structure formation, the re-ionization of baryonic matters in clusters is practically achieve at $z \sim 6$ when the dark matter haloes began to collapse. In the redshift range [2,6], (relatively) dense and hot gas structures should already exist. Even if they are not as massive as closer structure. Individual detection is not possible, a **statistical approach** is required.
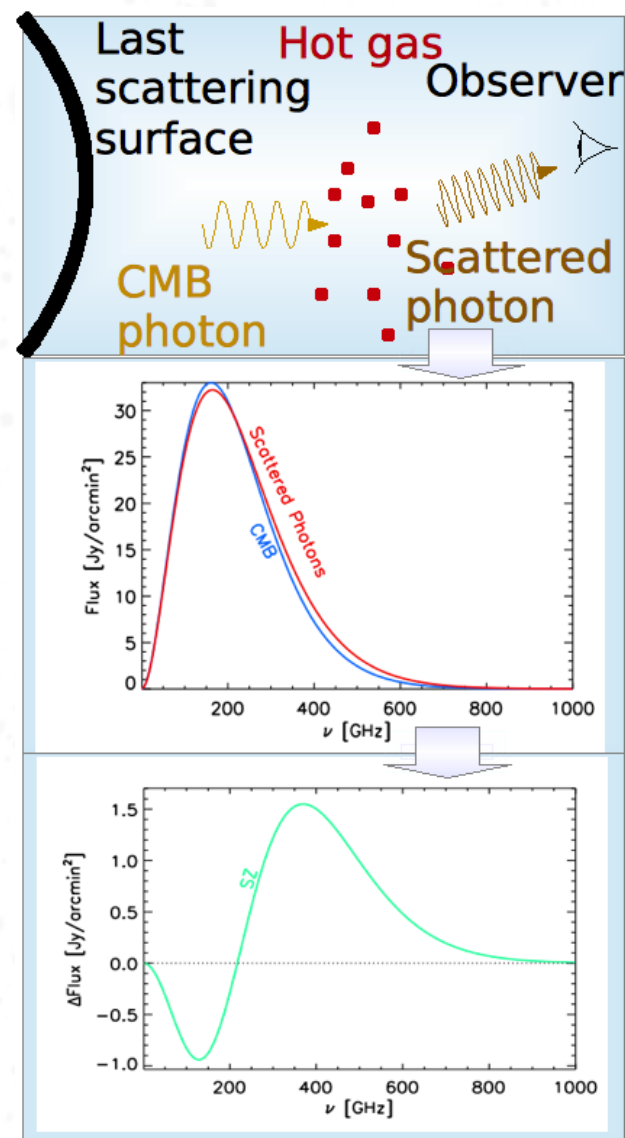
Detection of hot gas at higher redshift (z>1)

Individual detection at low redshift

Individual detection of clusters is possible for low-redshift structures via the X-ray Bremsstrahlung and the millimeter wavelength Sunyaev-Zel'dovich effect. Some actual limits:

- millimeter wavelength: SPT survey: detection of clusters up to z=1.5
- X-ray: Chandra confirmed a cluster at z=1.8 Links: http://arxiv.org/abs/1311.4361

More distant structures

In the standard model of structure formation, the re-ionization of baryonic matters in clusters is practically achieve at $z \sim 6$ when the dark matter haloes began to collapse. In the redshift range [2,6], (relatively) dense and hot gas structures should already exist. Even if they are not as massive as closer structure. Individual detection is not possible, a **statistical approach** is required.

How to proceed?

- We want to detect the hot gas using the **Sunyaev-Zel'dovich effect**. We use the Planck maps at seven frequencies.
- We need an **independent tracer** for the hot gas. We use the quasars from the SDSS survey and look at the positions of them on the Planck maps. Quasars are very bright galaxies, and are supposed to be created and to live in relatively dense environment on average. SDSS quasars have a redshift range from 0.1 to 6.44.
- Basically, we obtain a flux at each quasar's position with a match filter. To increase the signal-to-noise, we work with the **average flux**.

Table of contents

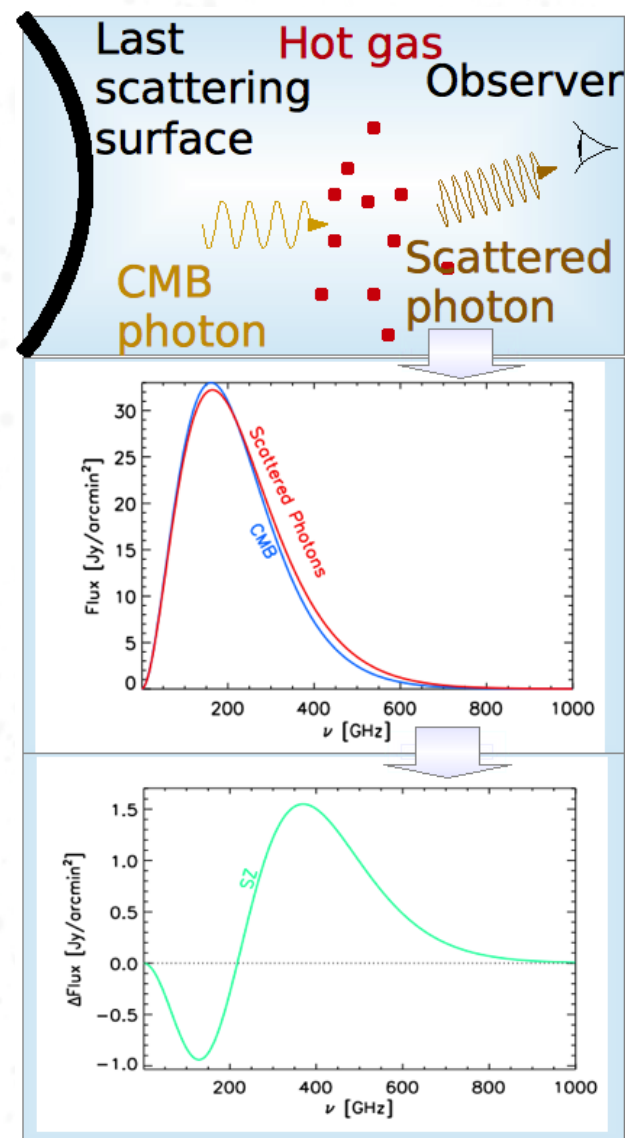# The Sunyaev-Zel'dovich effect

Sunyaev-Zel'dovich detection

The hot gas inside the intra-cluster medium scatters the photons from the cosmic microwave background and changes their spectrum via **inverse Compton scattering**. That's the Sunyaev-Zel'dovich (SZ) effect which is mainly in the millimeter wavelength range.

The millimeter wavelength sky maps from the PLANCK data are well-suited for the SZ detection of the hot gas.

The Sunyaev-Zel'dovich effect

Sunyaev-Zel'dovich detection

The hot gas inside the intra-cluster medium scatters the photons from the cosmic microwave background and changes their spectrum via **inverse Compton scattering**. That's the Sunyaev-Zel'dovich (SZ) effect which is mainly in the millimeter wavelength range.

The millimeter wavelength sky maps from the PLANCK data are well-suited for the SZ detection of the hot gas.

Interesting properties

The shape of the SZ effect doesn't depends on the redshift of the cluster, on its spatial extent, on its mass or on its Temperature. Only the amplitude, the **Compton parameter**, depends on them.
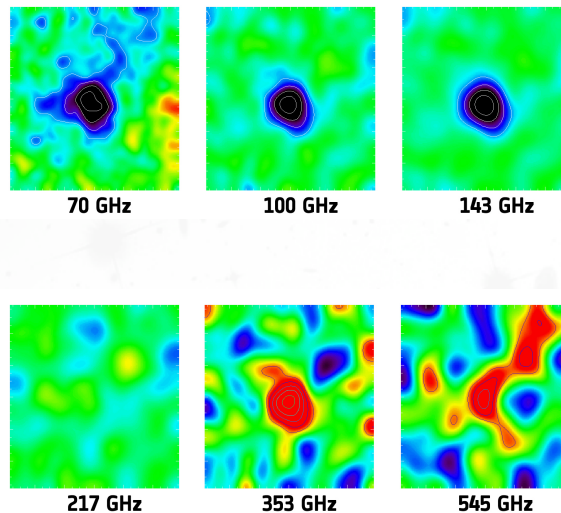
Table of contents

Mono frequency filtering approach

Main goal

First step: we want to determine the nature of our signal at the quasar's position, i. e., its frequency dependence.

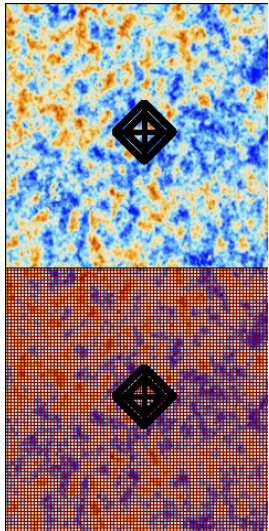# Mono frequency filtering approach

Main goal

First step: we want to determine the nature of our signal at the quasar's position, i. e., its frequency dependence.

Formal description of a Planck map

$m_\nu(\vec{x}) = F_\nu \cdot \tau_\nu(\vec{x} - \vec{x_0}) + n_\nu(\vec{x})$ with

- $m_\nu(\vec{x})$, the Planck map at $\vec{x} = (RA, DEC)$,
- F_ν, the flux from the structure (quasar and hot gas),
- $\vec{x_0}$ the quasar's position,
- $\tau_\nu(\vec{x})$ the spatial profile of the cluster (convolved with the Planck beam) and
- $n_\nu(\vec{x})$ the instrumental and astrophysical noise.

We want F_ν for each quasar.

Mono frequency filtering approach

Main goal

First step: we want to determine the nature of our signal at the quasar's position, i. e., its frequency dependence.

Formal description of a Planck map

$m_\nu(\vec{x}) = F_\nu \cdot \tau_\nu(\vec{x} - \vec{x_0}) + n_\nu(\vec{x})$ with

- $m_\nu(\vec{x})$, the Planck map at $\vec{x} = (RA, DEC)$,
- F_ν, the flux from the structure (quasar and hot gas),
- $\vec{x_0}$ the quasar's position,
- $\tau_\nu(\vec{x})$ the spatial profile of the cluster (convolved with the Planck beam) and
- $n_\nu(\vec{x})$ the instrumental and astrophysical noise.

We want F_ν for each quasar.

Mono-frequency filter

We employ a mono-frequency matched filter $\Psi_\nu(\vec{x})$ to estimate quasar flux $F_\nu = w(\vec{x_0})$ with $w_\nu(\vec{x}) = \int d^2x' \, \Psi_\nu(\vec{x'} - \vec{x}) m_\nu(\vec{x'})$ the filtered flux map. The filter is suited to give a **non biased flux** at the **best signal-to-noise ratio** assuming the cluster profile $\tau_\nu(\vec{x})$.

Table of contents

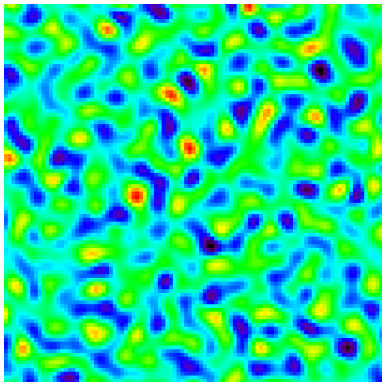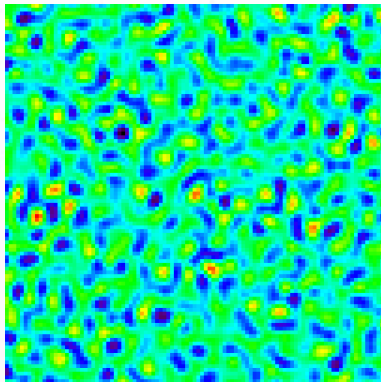# Average flux

For each quasar, the flux is under the noise. We must work with the average values for the whole quasar population, so ~ 280000 positions. We present here the average filtered maps centered on the quasar's positions.
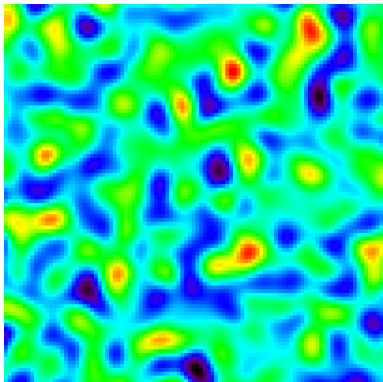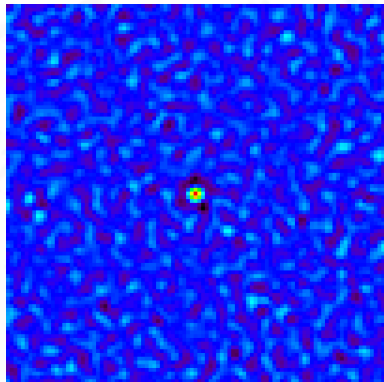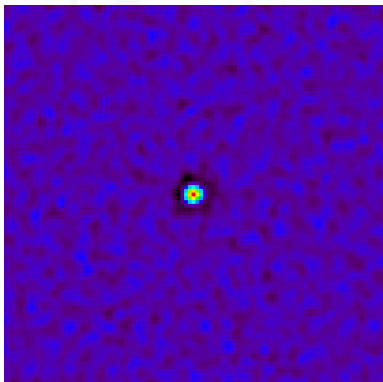

Average filtered map at 70 GHz
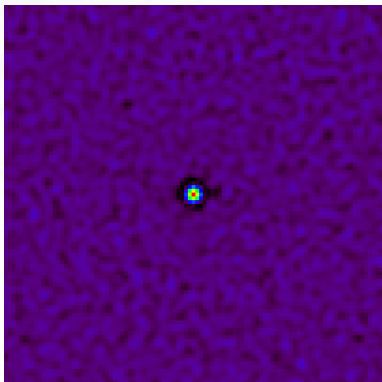

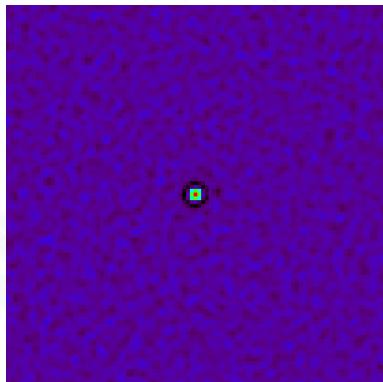Average filtered map at 100 GHz

Average filtered map at 143 GHz

Average filtered map at 217 GHz

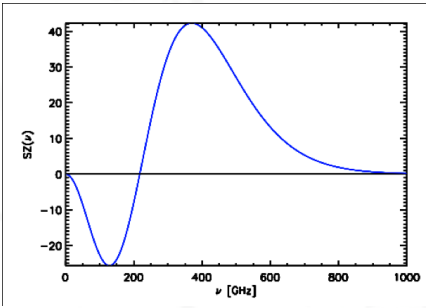Average filtered map at 353 GHz
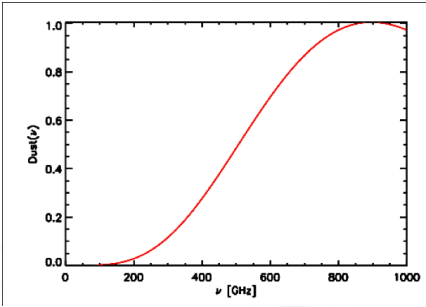

Average filtered map at 545 GHz

Average filtered map at 857 GHz
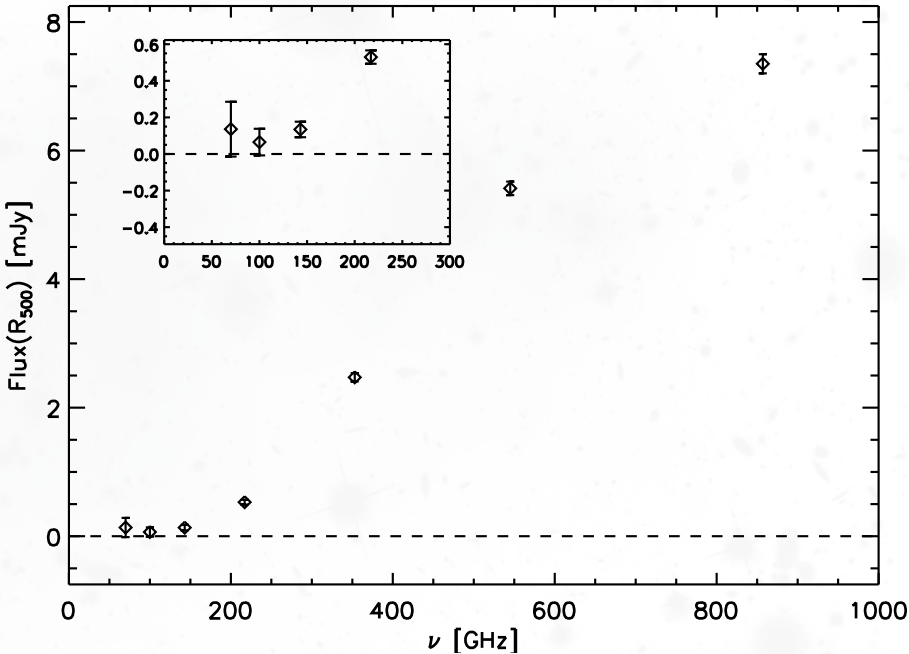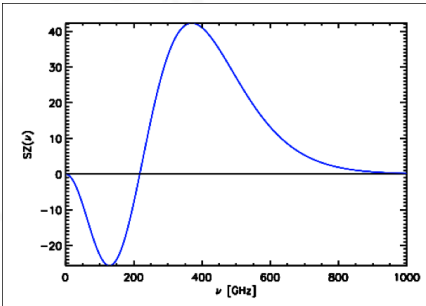
Average flux

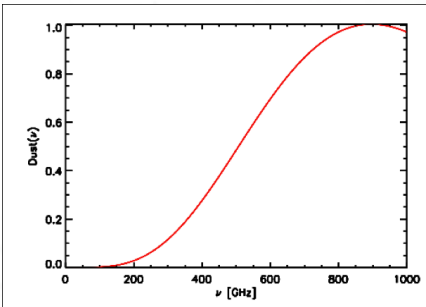SZ spectra

Dust modeled as a grey body

Dusty signal

The average flux is closer to a grey body spectrum than the expected SZ spectrum. A grey body is a black body times a power law $dust(T_{dust}, \beta, \nu) = B_\nu(T_{dust}) \cdot (\nu/\nu_0)^\beta$ and is associated with emissions from grains of dust heated by stars. So, the signal is **dominated by the dust emissions**, probably from the host galaxies of the quasars.

Average flux

SZ spectra

Dust modeled as a grey body

Dusty signal

The average flux is closer to a grey body spectrum than the expected SZ spectrum. A grey body is a black body times a power law $dust(T_{dust}, \beta, \nu) = B_\nu(T_{dust}) \cdot (\nu/\nu_0)^\beta$ and is associated with emissions from grains of dust heated by stars. So, the signal is **dominated by the dust emissions**, probably from the host galaxies of the quasars.
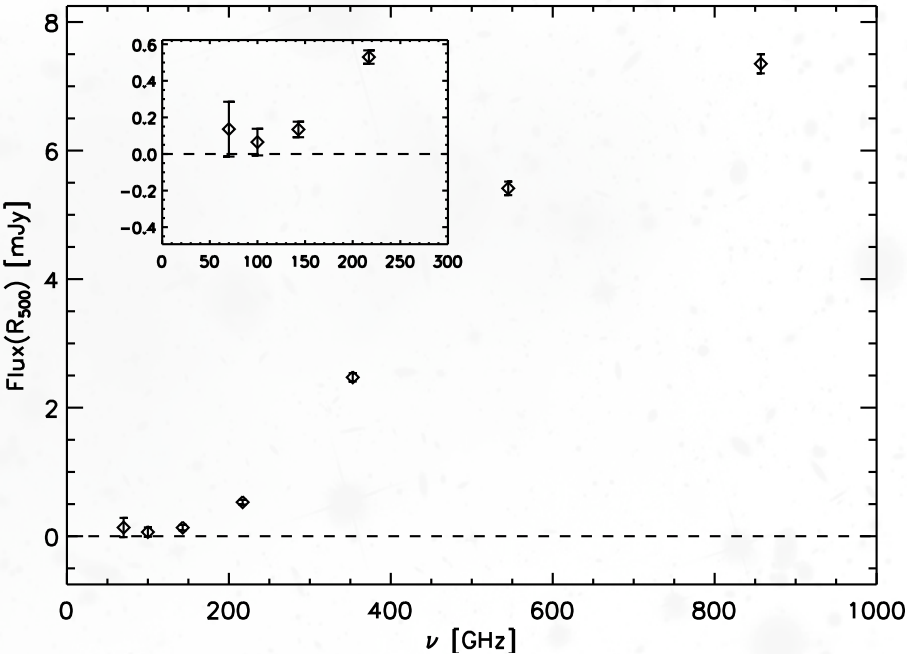
And next?

If we want to have a chance to detect a SZ signal, we have to understand the dominant dust signal. Dust emission is parametrized by a temperature T_{dust} and a slope β. We must find the best values of these parameters.

Table of contents
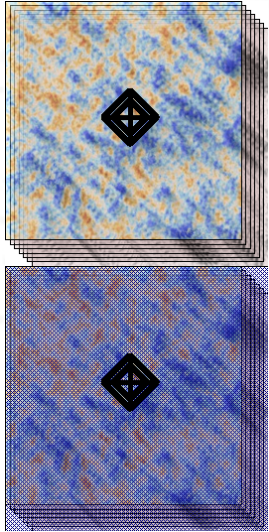
Multi frequency filtering approach

Hypothesis on the flux

We assume that the flux have a **frequency dependance** with a given amplitude A so that $F_\nu = A \cdot E(\nu)$. Our first hypothesis is to consider the flux to be dust signal only. We write $F_\nu = D \cdot dust(T_{dust}, \beta, \nu)$ with D the amplitude of the dust.

Multi frequency filtering approach

Hypothesis on the flux

We assume that the flux have a **frequency dependance** with a given amplitude A so that $F_\nu = A \cdot E(\nu)$. Our first hypothesis is to consider the flux to be dust signal only. We write $F_\nu = D \cdot dust(T_{dust}, \beta, \nu)$ with D the amplitude of the dust.

Multi-frequency filter

Now, we employ a multi-frequency matched filter $\vec{\Psi}(\vec{x})$ to estimate the amplitude $A = w(\vec{x_0})$ with $w(\vec{x}) = \int d^2 x' \, \vec{\Psi}(\vec{x'} - \vec{x}) \cdot \vec{m}(\vec{x'})$ the filtered amplitude map. This new filter **combine the data at several frequencies** to maximize the signal-to-noise ratio. To use it, we have to assume a frequency dependence for the signal.
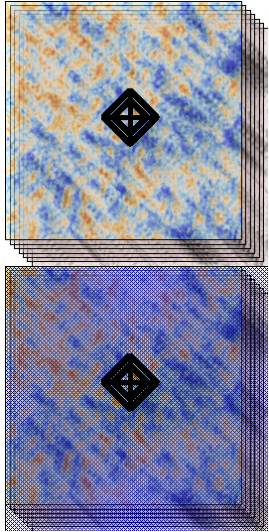
Multi frequency filtering approach

Hypothesis on the flux

We assume that the flux have a **frequency dependance** with a given amplitude A so that $F_\nu = A \cdot E(\nu)$. Our first hypothesis is to consider the flux to be dust signal only. We write $F_\nu = D \cdot dust(T_{dust}, \beta, \nu)$ with D the amplitude of the dust.

Multi-frequency filter

Now, we employ a multi-frequency matched filter $\vec{\Psi}(\vec{x})$ to estimate the amplitude $A = w(\vec{x_0})$ with $w(\vec{x}) = \int d^2x' \, \vec{\Psi}(\vec{x'} - \vec{x}) \cdot \vec{m}(\vec{x'})$ the filtered amplitude map. This new filter **combine the data at several frequencies** to maximize the signal-to-noise ratio. To use it, we have to assume a frequency dependence for the signal.

Residuals and χ^2

To check our hypothesis, we compare the flux F_ν from the match mono-frequency filter with the effective flux $A \cdot E(\nu)$ obtained with the matched multi-frequency filter thanks to the residuals $R_\nu = F_\nu - A \cdot E(\nu)$ From the residuals, we compute the χ^2. This χ^2 depends on the choice of the frequency dependence. Here it **depends on T_{dust} and** β.
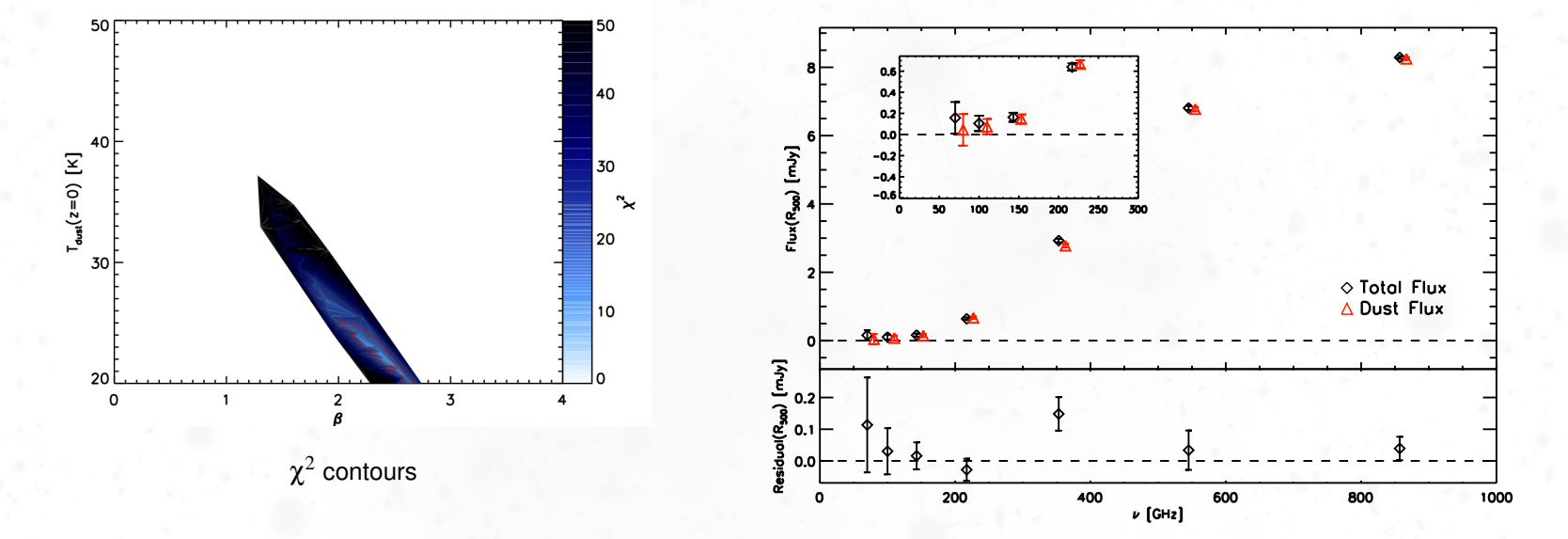
Table of contents

Features of the dust emission

Method

We fix T_{dust} and β. For each quasars, we obtain the flux at the different frequencies and the amplitude of the dust and find the residuals. We compute the average values and the χ^2. Then we proceed similarly for other values of T_{dust} and β. The χ^2 is **minimize** by a Powell algorithm. We find $T_{dust} = 21.823$ and $\beta = 2.446$ at our best point.

χ^2 contours

Top: Total flux (black) and dust flux(red) at the minimal χ^2. *Bottom:* residuals at the minimal χ^2
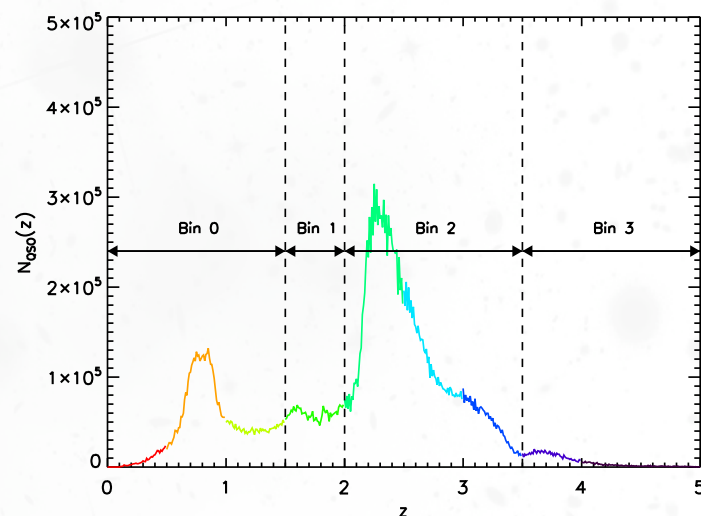
Table of contents

Dust evolution across redshift

Work on regular samples

We separate our quasars population in redshift bins with a regular redshift width of 0.5. For each bin, we minimize the χ^2 independently. Bins with close convergence area are merged into wider bins. Each large homogeneous population of quasars has different temperature T_{dust} and β.
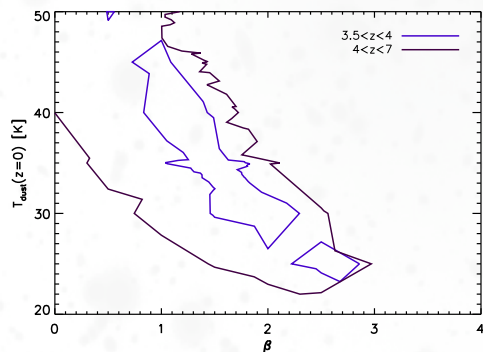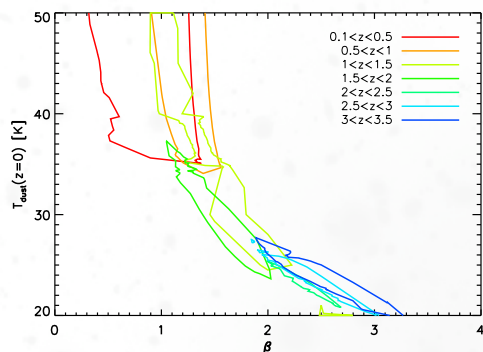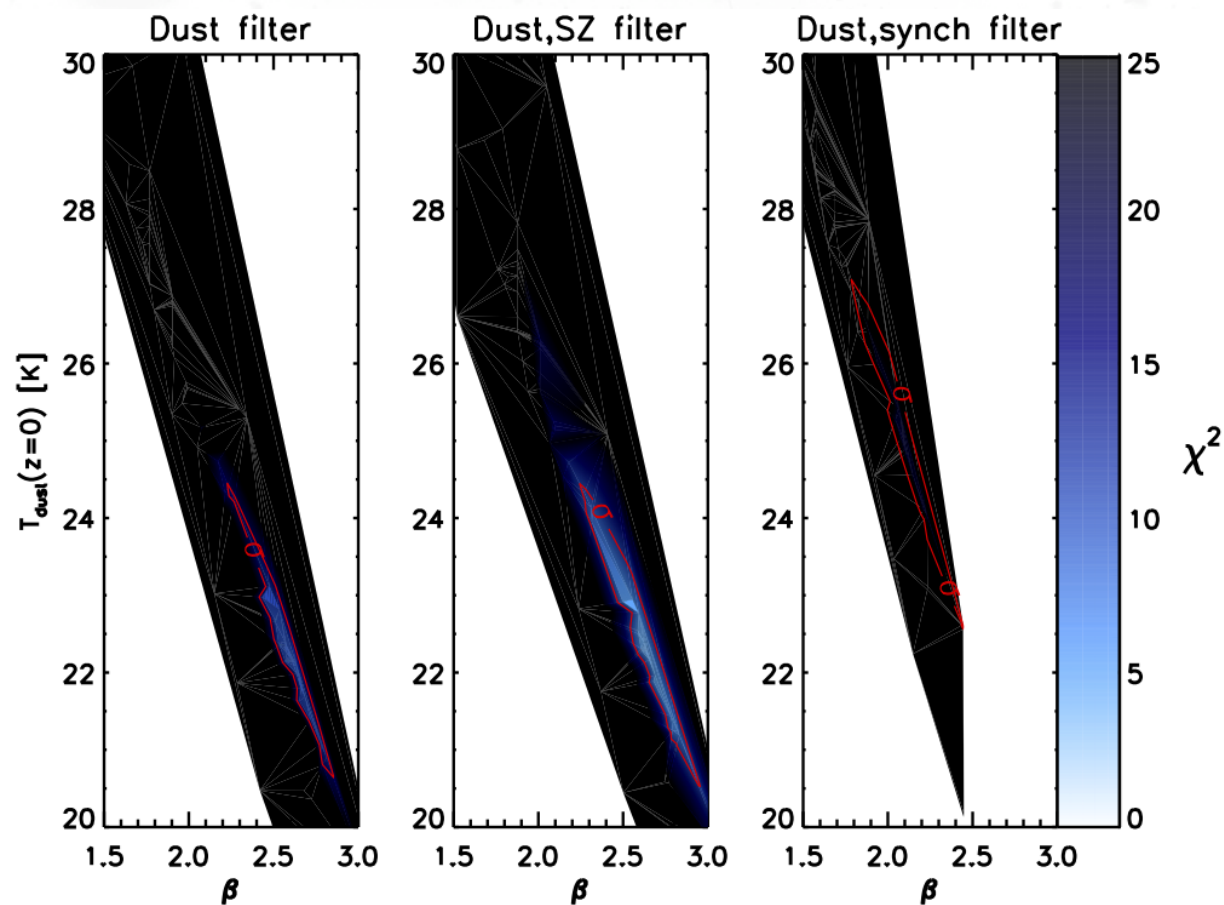

1 σ contours

quasars distribution

Table of contents

Detection of a signal from hot gas (Finally !)

Where do we find it?

The most promising sample for the SZ signal is the bin $z \in [2, 3.5]$ of quasars without radio counterpart. Quasars with radio counterpart strongly contaminate the signal with a synchrotron (power-law) emission. We suppose the flux having two components, a dust component and a SZ component, so $F_\nu = D \cdot dust(T_{dust}, \beta, \nu) + y \cdot SZ(\nu)$ with y the Compton parameter. A **linear combination of multi-frequency filter** is used here to separate the two components.

χ^2 contours for different filters

Detection of a signal from hot gas (Finally !)

Where do we find it?

The most promising sample for the SZ signal is the bin $z \in [2, 3.5]$ of quasars without radio counterpart. Quasars with radio counterpart strongly contaminate the signal with a synchrotron (power-law) emission. We suppose the flux having two components, a dust component and a SZ component, so $F_\nu = D \cdot dust(T_{dust}, \beta, \nu) + y \cdot SZ(\nu)$ with y the Compton parameter. A **linear combination of multi-frequency filter** is used here to separate the two components.
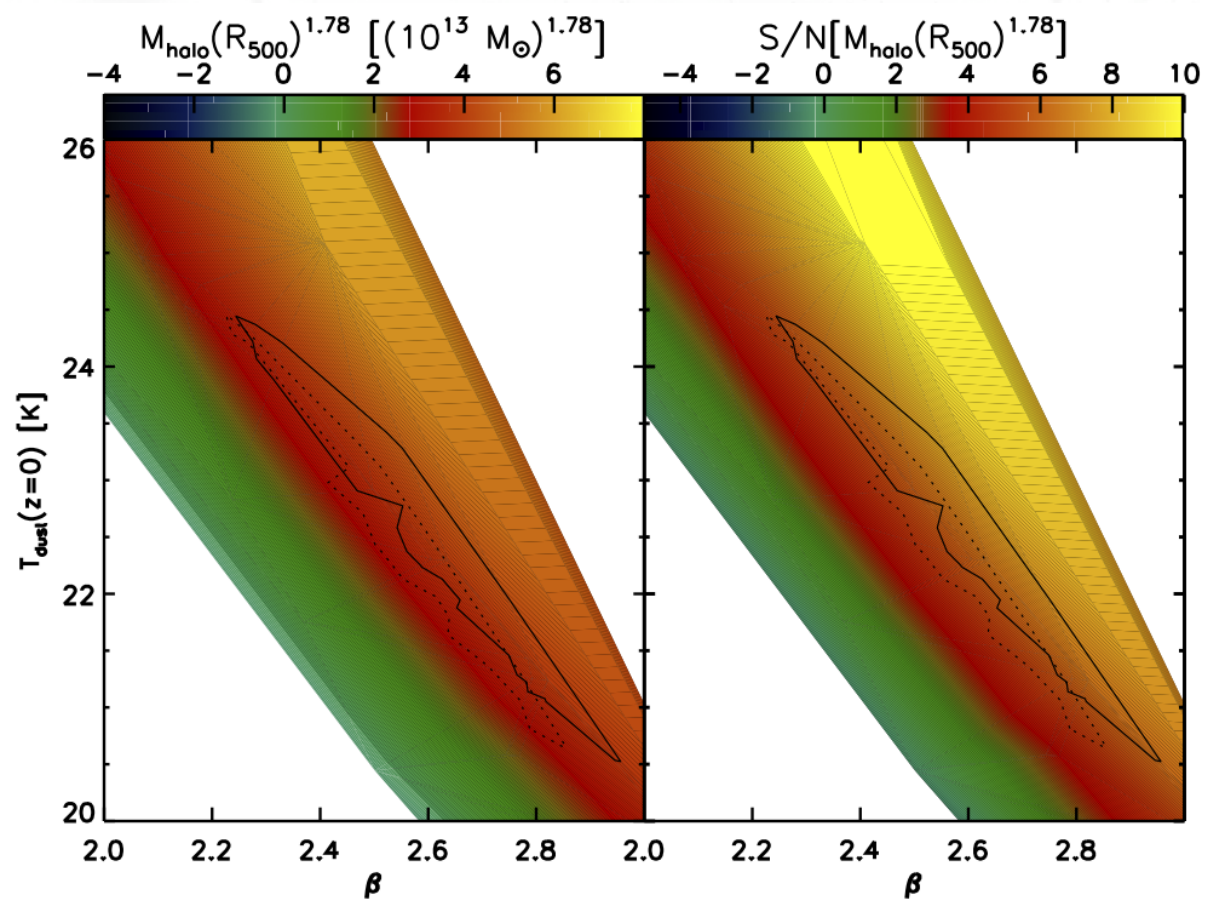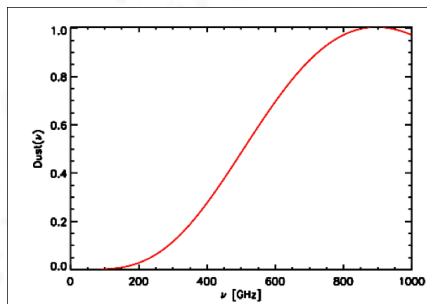

Evolution of total halo mass estimation (computed from y) and its signal-to-noise ration in T_{dust}, β plane.

Table of contents

To conclude

Dust signal is dominant

At the positions of the quasars on the Planck map, **the dominant emission comes from dust** and not from the SZ effect. In order to find an SZ signal, we have to fit the dust emission for the whole quasars population and for redshift samples. The filtering on the last suggests **an evolution of the parameters T_{dust}, β across the redshift.**
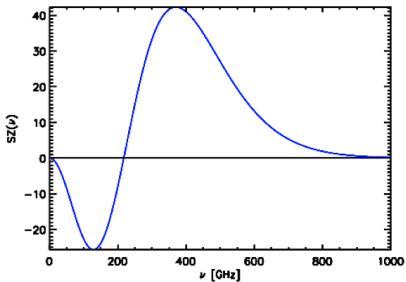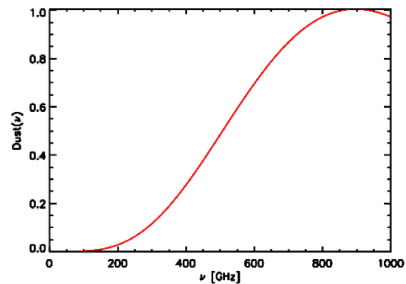
To conclude

Dust signal is dominant

At the positions of the quasars on the Planck map, **the dominant emission comes from dust** and not from the SZ effect. In order to find an SZ signal, we have to fit the dust emission for the whole quasars population and for redshift samples. The filtering on the last suggests **an evolution of the parameters T_{dust}, β** across the redshift.

Evidence for hot gas in high redshift structures

In addition of the dust emission, there is strong evidence for a **SZ signal** at the positions of quasars with $z \in [2, 3.5]$ and with no radio counterpart:

- the dust + SZ filtering gives the minimal χ^2,
- the SZ signal is robust in the convergence valley and its signal-to-noise ratio is also robust there.

Thanks for your attention!

Annexe: The χ^2 distribution

Samples and method

We build 180 sub-samples of 2000 quasars with random positions on the sky. At these positions, we inject a flux on the Planck maps to create the injected Planck map. In the first case, flux is a dust signal and we employ a dust filter. In the other case, it's a dust and SZ signal and we employ the dust + SZ filter. For each sub-sample, for both filters, we compute two χ^2: the first at the T_{dust} and β (fixed) of the injection and the second via a Powell algorithm (variable parameters). Both filters have the **same χ^2 distribution**.
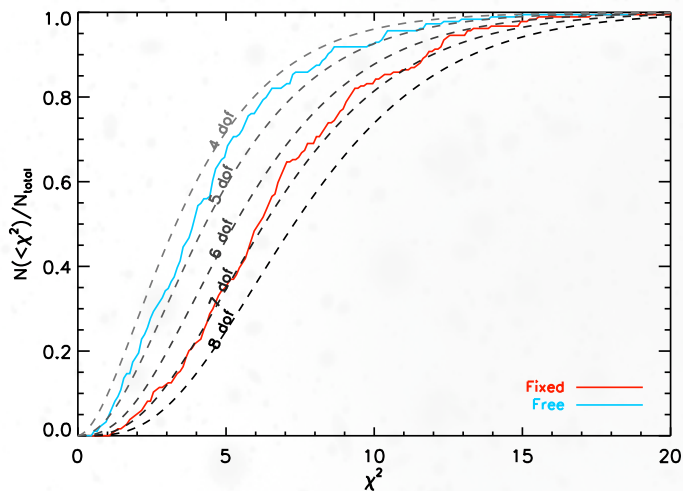
χ^2 distribution for dust filtering of dust emission
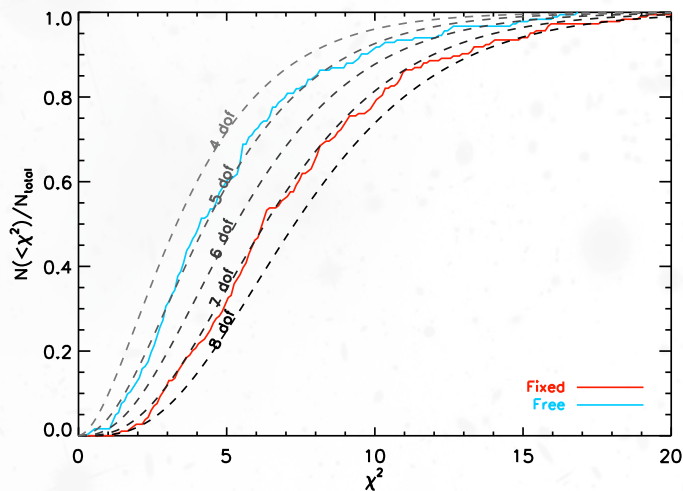
χ^2 distribution for dust + SZ filtering of dust + SZ emission